4. M. H. Greenblatt and P. A. Miller, Jr., "A Microwave Secondary-Electron Multiplier," *Phys. Rev., Vol. 72*, p. 160 (1947)
5. M. H. Greenblatt, "On the Measurement of the Average Time Delay in Secondary Emission," *RCA Rev., Vol. 16*, p. 52 (1955)
6. C. G. Wang, "Reflex Oscillators Using Secondary-Emission Current," *Phys. Rev., Vol. 68*, p. 284 (1945)
7. E. W. Ernst and H. Von Foerster, "Time Dispersion of Secondary Electron Emission," *J. Appl. Phys., Vol. 26*, p. 781 (1955)
8. E. O. Lawrence and J. W. Beams, "Instantansity of the Photoelectric Effect," *Phys. Rev., Vol. 29*, p. 903 (1927)
9. M. Birk, Q. A. Kerns, and R. F. Tusting, "Evaluation of the C-70045A High-Speed Photomultiplier," *IEEE Trans. Nucl. Sci. Vol. NS-11*, p. 129 (1964)

Principles of Photomultiplier Design

THIS section describes the physical and electrical parameters of interest in the design of photomultipliers. The effects of dynode and anode structures on such parameters as time response, sensitivity, and dark current are discussed. A section covering ruggedized photomultipliers describes their structure and method of testing.

PHOTOCATHODE-TO-FIRST DYNODE REGION

As mentioned in the preceding section, two classes of photocathodes are used in photomultipliers: opaque and semitransparent. Because opaque photocathodes are an integral part of the electron-multiplier structure, they are discussed later in connection with the electron multiplier. Semitransparent photocathodes are formed on planar or spherical-section windows which are part of the photocathode-to-first dynode region. Semitransparent photocathodes have large, readily accessible light-collection areas which may be directly coupled to scintillation crystals.

A planar-photocathode design, such as that shown in Fig. 12(a), provides excellent coupling to a scintillation crystal, but its time response is not as good as that of a spherical-section photocathode. The spherical-section photocathode shown in Fig. 12(b) when coupled to a high-speed electron multiplier provides a photomultiplier having a very fast time response. Some tube types utilize a spherical-section photocathode on a plano-concave faceplate to facilitate scintillator coupling. This design is usually limited to faceplate diameters of two inches or less because of the excessive thickness of the glass at the edge. The plano-concave faceplate may also contribute to some loss in uniformity of sensitivity because of internal reflection effects near the thick edge of the photocathode.

Design Analysis

Photocathode-to-first-dynode structures are usually axially symmetric, with the symmetry axis passing through the center of the photocathode. This symmetry simplifies the electron-optical analysis of the photocathode-to-first-dynode region because the problem is reduced from three dimensions to two. The first step in the analysis is the solution of the Laplace equation, $\nabla^2 V = 0$. Because a solution of this equation in closed form is impossible for most geometries, numerical solutions are obtained;[1] one solution[2] results in the photocathode-to-first-dynode region shown in Fig. 12(b). Performance is determined by use of a computer to trace equipotential lines and electron trajectories which can

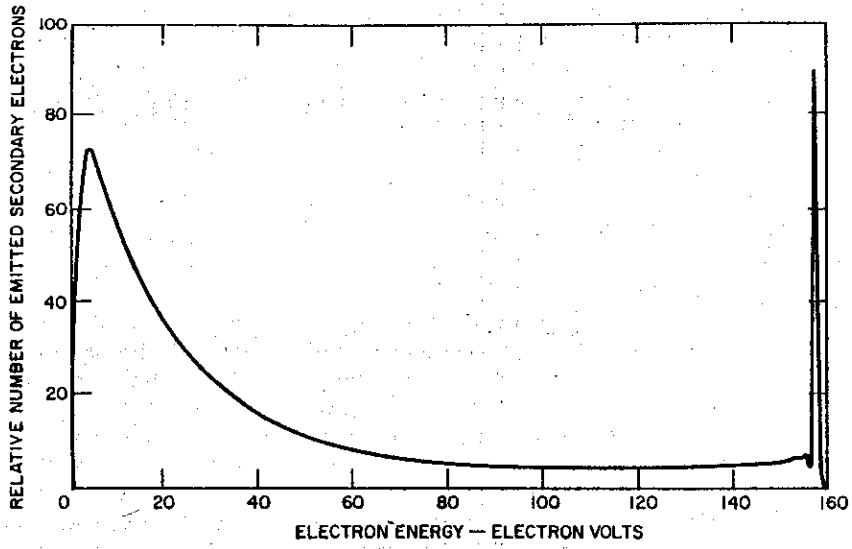

Fig. 11 — Typical secondary-electron energy distribution; peak at right is caused by reflected primary electrons.

curve does not represent a true secondary, but rather a reflected primary. Data are not available for the emission energies from a negative-electron-affinity material, but they are expected to be considerably less than for positive-affinity materials.

Negative electron affinity has not only expanded the field of photoemission, but has proved very important in the development of greatly improved secondary-emitting materials for use as dynodes in photomultipliers. With negative-electron-affinity materials, such as GaP, the secondary-emission ratio increases almost linearly up to very high primary energies; factors up to 130 have been measured. This factor compares with typical values of less than 10 for previously used dynode materials.

Effects of Secondary-Emission Statistics

The statistical distribution of secondary-emission yields tends to degrade the signal-to-noise ratio in a photomultiplier; the greatest contribution to the noise occurs at the first dynode. If the secondary-emission ratio of the first dynode is improved through the use of a negative-electron-affinity material, such as GaP, the emission statistics of the first dynode are markedly improved and the performance of the multiplier more closely resembles that of a perfect amplifier. Photomultiplier statistics are explained in greater detail in the section on **Statistical Fluctuation and Noise.**

The incorporation of high-gain secondary-emission materials throughout the dynode chain makes it possible to design photomultipliers with fewer stages for given amplifications. The use of fewer stages also reduces the variation of gain with voltage changes.

Time Lag in Photoemission and Secondary Emission

Because both photoemission and secondary emission can be described in terms of the excitation of electrons within the volume of the solid and the subsequent diffusion of these electrons to the surface, a finite time interval occurs between the instant that a primary (photon or electron) strikes a surface and the emergence of electrons from the surface. Furthermore, in the case of secondary emission, the secondaries can be expected to reach the surface over a period of time. Within the limitations of a mechanistic approach to a quantum phenomenon, time intervals for metals or insulators of the order of 10^{-13} to 10^{-14} second may be estimated from the known energy of the primaries, their approximately known range, and the approximately known diffusion velocities of the internal electrons. In negative-electron-affinity semiconductors, it is known that the lifetime of internal "free" electrons having quasi-thermal energies (i.e. electrons near the bottom of the conduction band) can be of the order of 10^{-10} second.

Thus far experiments have provided only upper limits for the time lag of emission. In the case of secondary emission, a variety of experiments have established limits. Several investigators [3, 4, 6] have deduced limits from the measured performance of electron tubes using secondary emitters. Others, making direct measurements of these limits, determined the time dispersion of secondary emission by letting short electron bunches strike a target and comparing the duration of the resulting secondary bunches with the measured duration of the primary bunch. By this means an upper limit of 6×10^{-12} second was determined for platinum [7] and an upper limit of 7×10^{-11} second for an MgO layer [5] formed on the surface of an AgMg alloy.

The upper limit for the time lag in photoemission, however, is not well established. One investigation [8] determined a limit of 3×10^{-9} second. From careful measurements [9] of the time performance of fast photomultipliers it can be inferred that the limit must be at least an order of magnitude smaller.

While these limits are a useful guide to the type of time performance to be expected in present photomultipliers, they will probably have less significance as new photomultipliers using semiconducting photoemitters and secondary emitters are developed. Semiconductors having minority-carrier lifetimes of the order of microseconds are now available. Probably, by combination of this characteristic with negative electron affinity, higher gains and quantum efficiencies can be achieved, but at a sacrifice of time response or band width. However, the first generation of negative-electron-affinity emitters (e.g., GaP) has actually resulted in photomultipliers having better time performance because a smaller number of stages operating at higher voltage can be used. At this time it can only be concluded that in the future photomultipliers will probably be designed to match in more detail the requirements of a particular use.

REFERENCES

1. A. H. Sommer, *Photoemissive Materials*, John Wiley, New York (1968)
2. R. E. Simon and B. F. Williams, "Secondary Electron Emission," *IEEE Trans. Nucl. Sci., Vol. NS–15*, No. 3, p. 167 (1968)
3. G. Diemer and J. L. H. Jonker, "On the Time Delay of Secondary Emission," *Philips Research Repts., Vol. 5*, p. 161 (1950)

1. The incident electrons interact with electrons in the material and excite them to higher energy states.
2. Some of these excited electrons move toward the vacuum-solid interface.
3. Those electrons which arrive at the surface with energy greater than that represented by the surface barrier are emitted into the vacuum.

When a primary beam of electrons impacts a secondary-emitting material, the primary-beam energy is dissipated within the material and a number of excited electrons are produced within the material. Based on experimental data, approximations have been made [2] based on the assumption that the range of primary electrons varies as the 1.35 power of the primary energy and that the number of electrons excited is uniform throughout the primary range. The numbers of excited electrons produced are indicated in Fig. 9 for primary energies varying from 400 to 2200 electron-volts. The total number of excited electrons produced by a primary is indicated by the area of the individual rectangles in the figure.

As an excited electron in the bulk of the material moves toward the vacuum-solid interface, it loses energy as a result of collisions with other electrons and optical phonons. The energy of the electron is very rapidly dissipated as a result of these collisions, and it is estimated that the energy of such an electron will decay to within a few times the mean thermal energy above the bottom of the conduction band within 10^{-12} second. If the electron arrives at the vacuum-solid interface with energy below that required to traverse the potential barrier, it cannot escape as a secondary electron. Therefore, only those electrons excited near the surface of the material are likely to escape as secondary electrons. The probability of

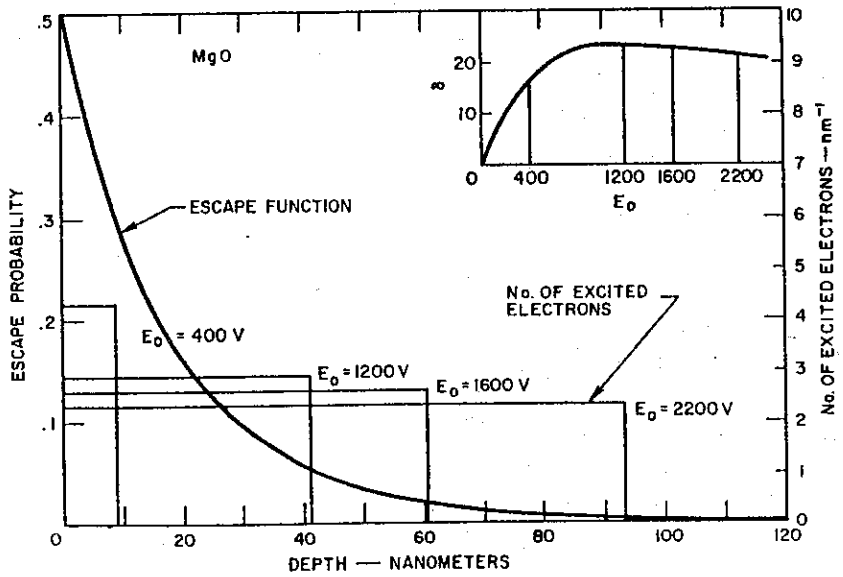

Fig. 9 — An illustration showing the processes of secondary emission. See text for explanation.

escape for an excited electron is assumed to vary exponentially with the excitation depth, as indicated in Fig. 9. If the product of the escape function and the number of excited electrons (which is a function of primary energy and depth) is integrated, a secondary-emission-yield function may be obtained, as indicated in the insert at the top of Fig. 9. The model which has been assumed thus explains the general characteristics of secondary emission as a function of primary energy. Secondary-emission yield increases with primary energy, provided the excited electrons are produced near the surface where the escape probability is high. As the primary-electron energy increases, the number of excited electrons also increases, but the excitation occurs at greater depths in the material where escape is much less probable. Consequently, the secondary-emission yield eventually reaches a maximum and then decreases with primary energy.

Experimental secondary-emission-yield values are shown as a function of primary-electron energy in Fig. 10 for MgO, a traditional secondary-emission material, and for GaP(Cs), a recently developed negative-electron-affinity material. Although both of these materials display the general characteristics of secondary emission as a function of primary energy, as expected from the model illustrated in Fig. 8, the secondary-emission yield for GaP(Cs) increases with voltage to much higher values. Even though electrons are excited rather deep in the negative-electron-affinity material and lose most of their excess energy as a result of collisions, many still escape into the vacuum because of the nature of the surface barrier.

When secondary electrons are emitted into the vacuum, the spread of emission energies may be quite large, as illustrated in the curve of Fig. 11 for a positive-affinity emitter. The peak at the right of the

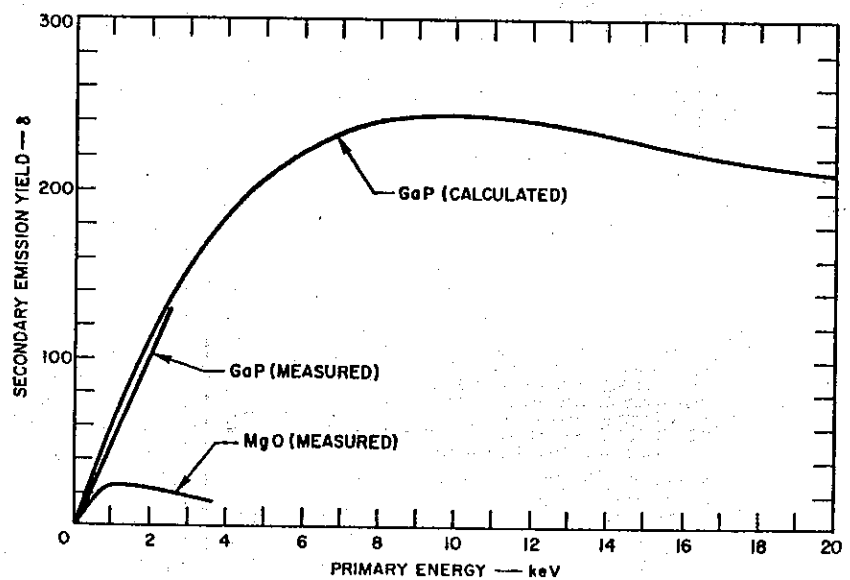

Fig. 10 — Typical curve of secondary-emission yield as a function of primary-electron energy in GaP(Cs) and MgO.

Table I — *Nominal Composition and Characteristics of Various Photocathodes.*

Nominal Composition	Response Designation	Type of Photocathode	Envelope Material[a]	Conversion Factor[b] (lumen/watt at λmax)	Luminous Sensitivity (μA/lumen)	Wavelength of Maximum Response, λmax (nm)	Sensitivity at λmax (mA/watt)	Quantum Efficiency at λmax (percent)	Dark Emission at 25°C A x 10^{-15}/cm²
Ag-O-Cs	S-1	O	0080	92.7	25	800	2.3	0.36	900
Ag-O-Rb	S-3	O	0080	285	6.5	420	1.8	0.55	—
Cs_3Sb	S-19	O	SiO_2	1603	40	330	64	24	0.3
Cs_3Sb	S-4	O	0080	1044	40	400	42	13	0.2
Ca_3Sb	S-5	O	9741	1262	40	340	50	18	0.3
Cs_3Bi	S-8	O	0080	757	3	365	2.3	0.77	0.13
Ag-Bi-O-Cs	S-10	S	0080	509	40	450	20	5.6	70
Cs_3Sb	S-13	S	SiO_2	799	60	440	48	14	4
Cs_3Sb	S-9	S	0080	683	30	480	20	5.3	—
Cs_3Sb	S-11	S	0080	808	60	440	48	14	3
Cs_3Sb	S-21	S	9741	783	30	440	23	6.7	—
Cs_3Sb	S-17	O[g]	0080	667	125	490	83	21	1.2
Na_2KSb	S-24	S	7056	1505	32	380	64	23	0.0003
K-Cs-Sb	—	S	7740	1117	80	400	89	28	0.02
$(Ca)Na_2KSb$	—	S	SiO_2	429	150	420	64	18.9	0.4
$(Cs)Na_2KSb$	S-20	S	0080	428	150	420	64	19	0.3
$(Cs)Na_2KSb$	S-25	S	0080	276	160	420	44	13	—
$(Cs)Na_2KSb$	ERMA[c]	S	7056	169	265	575	45	10	1
Ga-As	—	O[h]	9741	148	250	450	37	10	0.1
Ga-As-P	—	O[i]	Sapphire	310	200	450	61	17	0.01
InGaAs-CsO[d]	—	O[h]	0080	266	260	400	71	22	1[d]
Cs_2Te	—	S	LiF	[e]	[e]	120	12.6	13	[f]
CsI	—	S	LiF	[e]	[e]	120	24	20	[f]
CuI	—	S	LiF	[e]	[e]	150	13	10.7	[f]

[a] Numbers refer to the following glasses:
0080—Corning Lime Glass
9741—Corning Ultraviolet Transmitting Glass
7056—Corning Borosilicate Glass
7740—Corning Pyrex Glass
SiO_2—Fused Silica (Suprasil—Trademark of Englehard Industries, Inc., Hillside, New Jersey)

[b] These conversion factors are the ratio of the radiant sensitivity at the peak of the spectral response characteristic in amperes per watt to the luminous sensitivity in amperes per lumen for a tungsten test lamp operated at a color temperature of 2854°K.

[c] An RCA designation for "Extended-Red Multialkali."

[d] An experimental photocathode, private communication from B. F. Williams, RCA Laboratories, Princeton, New Jersey. The dark emission indicated is a calculated value based on a bandgap of 1.1 eV for the particular composition studied. See also B. F. Williams, "InGaAs-CsO, A Low Work Function (Less Than 1.0 eV) Photoemitter," Appl. Phys. Letters 14, No. 9, p. 273 (1969).

[e] Not relevant.

[f] Data unavailable; expected to be very low.

[g] Reflecting substrate.

[h] Single crystal.

[i] Polycrystalline.

O = Opaque

S = Semitransparent

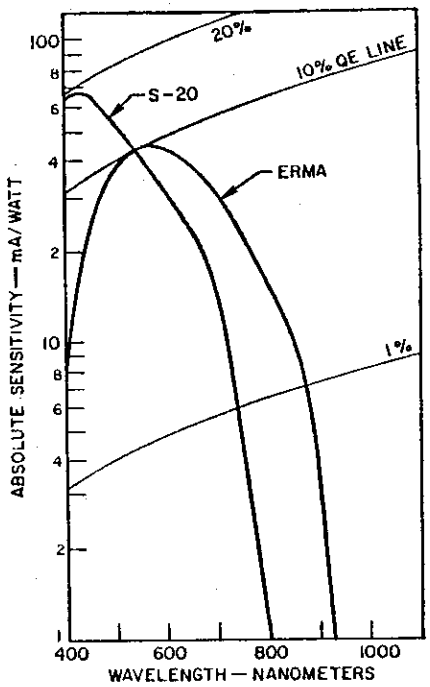

Fig. 7 — Typical spectral-response curve for one of the Extended Red Multi-Alkali (ERMA) photocathodes in comparison with a conventionally processed multialkali photocathode.

New Photocathode Materials

The negative-electron-affinity materials described earlier are used in opaque photocathodes. Typical spectral-response curves for GaAs(Cs) and $GaAs_xP_{1-x}(Cs)$ opaque photocathodes are shown in Fig. 8. Development of negative-electron-affinity materials is proceeding rapidly. Therefore, improved sensitivities and extended spectral ranges may be anticipated.

SECONDARY EMISSION

When electrons strike the surface of a material with sufficient kinetic energy, secondary electrons are emitted. The secondary-emission ratio or yield, δ, is defined as follows:

$$\delta = \frac{N_s}{N_e} \qquad (3)$$

where N_s is the average number of secondary electrons emitted for N_e primary electrons incident upon the surface.

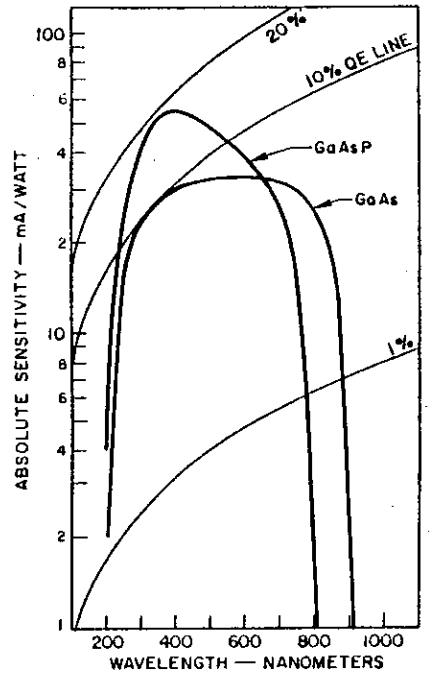

Fig. 8 — Typical spectral-response curves for GaAs(Cs) and $GaAs_xP_{1-x}(Cs)$ opaque photocathodes.

Fundamentals of Secondary Emission

The physical processes involved in secondary emission are in many respects similar to those already described under **Fundamentals of Photoemission.** The main difference is that the impact of primary electrons rather than incident photons causes the emission of electrons. The steps involved in secondary emission can be stated briefly as follows:

a single number to describe the response of the photocathode to some standard broad-band source, such as a tungsten lamp.

Variation in photocathode sensitivity over the range of wavelengths to which the photocathode material is sensitive is usually described by means of a spectral-response curve such as the one shown in Fig. 4. The abscissa may represent the wavelength in nanometers or angstroms, or the photon energy in electron-volts. The values can be converted from one scale to the other by use of Eq. 1.

The ordinate can also be expressed in many ways. The most common scale is amperes per incident watt, as shown; a second common scale is that of quantum efficiency, the average numbers of photoelectrons emitted per incident photon.

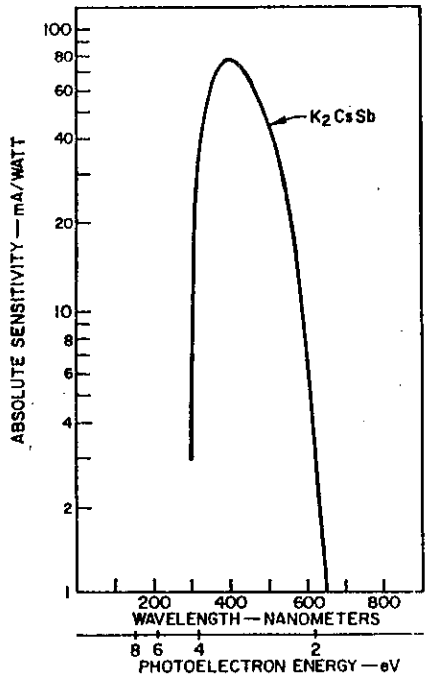

Fig. 4 — Typical spectral-response curve for a bialkali photocathode with a 008 lime-glass window.

It should be noted that the spectral response of photoemitters is modified by the window material. Therefore, the short-wavelength limit of the spectral response is generally a characteristic of the window rather than of the photocathode.

A common practice is to specify the response of the device to the incident flux from a tungsten lamp with a lime-glass window operating at a color temperature of 2854°K. The units of measurement are most frequently amperes per lumen. Sometimes sensitivity is expressed in terms of photocurrent and the total incident radiant power from the lamp on the photocathode window. This sensitivity is commonly stated in amperes per watt. It is the general practice to give sensitivity measurements in terms of incident flux. For some purposes, such as the study of photoemission phenomena, it may be useful to specify the sensitivity in terms of absorbed flux.

Opaque and Semitransparent Photocathodes

The photocathode consists of a material that emits electrons when exposed to radiant energy. There are two types of photocathodes. In one, the opaque photocathode, the light is incident on a thick photoemissive material and the electrons are emitted from the same side as that struck by the radiant energy. In the second type, the semitransparent photocathode, the photoemissive material is deposited on a transparent medium so that the electrons are emitted from the side of the photocathode opposite the incident radiation.

Because of the limited escape depth of photoelectrons, the thickness of the semitransparent photocathode film is critical. If the film

is too thick, much of the incident radiant energy is absorbed at a distance from the vacuum interface greater than the escape depth; if the film is too thin, much of the incident radiant energy is lost by transmission. Because radiant-energy absorption varies with wavelength, as shown in Fig. 5, the spectral response of a semitransparent photocathode can be controlled to some extent by control of its thickness. With increasing thickness, for example for alkali antimonides, blue response decreases and red response increases because of the difference in absorption coefficients.

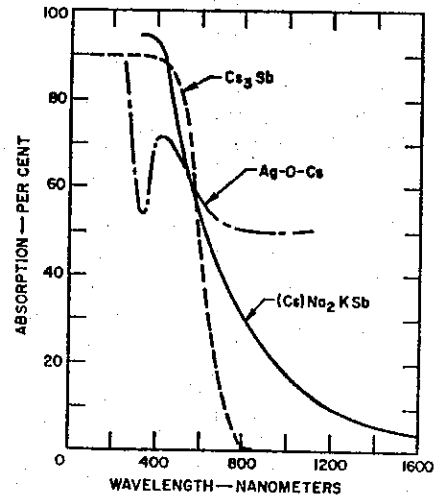

Fig. 5 — Radiation absorption for three commonly used semitransparent photocathode materials. Note loss of absorption in red region.

Photocathodes of Practical Importance

The photocathodes most commonly used in photomultipliers are silver-oxygen-cesium (Ag-O-Cs), cesium-antimony (Cs_3Sb), multialkali or trialkali [(Cs) Na_2KSb]*, and bialkali (K_2CsSb). Typical spectral-response curves for these materials are shown in Fig. 4 and Fig. 6. Additional information about these and other photocathodes of practical importance is shown in Table I.

The long-wavelength response of the multialkali photocathode has been extended recently by processing changes including the use of an increased photocathode-film thickness at the expense of the short-wavelength response. A typical spectral-response curve for one of these Extended Red Multi-Alkali (ERMA) photocathodes is shown in Fig. 7 in comparison with a conventionally processed multialkali photocathode.

* The parenthetical expression (Cs) indicates trace quantities of the element.

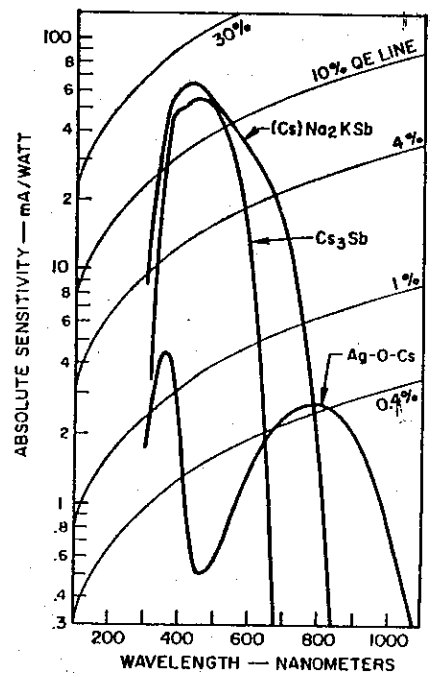

Fig. 6 — Typical spectral-response curves, with 008 lime-glass window, for (a) silver-oxygen-cesium (Ag-O-Cs), (b) cesium-antimony (Cs_3Sb), (c) multialkali or trialkali [(Cs)Na_2KSb].

equal to the band-gap energy E_G. If, as a result of light absorption, electrons are raised from the valence band into the conduction band, photoconductivity is achieved. For photoemission, an electron in the conduction band must have energy greater than the electron affinity E_A. The additional energy E_A is needed to overcome the forces that bind the electron to the solid, or, in other words, to convert a "free" electron within the material into a free electron in the vacuum. Thus, in terms of the model of Fig. 2, radiant energy can convert an electron into an internal photoelectron (photoconductivity) if the photon energy exceeds E_G and into an external photoelectron (photoemission) if the photon energy exceeds $(E_G + E_A)$. As a result, photons with total energies E_p less than $(E_G + E_A)$ cannot produce photoemission.

The following statements can therefore be made concerning photoemission in semiconductors. First, light absorption is efficient if the photon energy exceeds E_G. Second, energy loss by electron-electron scattering is low because very few free electrons are present; thus, energy loss by phonon scattering is the predominant loss mechanism. The escape depth in semiconductors is therefore much greater than in metals, typically of the order of tens of nanometers. Third, the threshold wavelength, which is determined by the work function in metals, is given by the value of $(E_G + E_A)$ in semiconductors. Synthesis of materials with values of $(E_G + E_A)$ below 2 electron-volts has demonstrated that threshold wavelengths longer than those of any metal can be obtained in a semiconductor. Semiconductors, therefore, are superior to metals in all three steps of the photoemissive process: they absorb a much higher fraction of the incident light, photoelectrons can escape from a greater distance from the vacuum interface, and the threshold wavelengths can be made longer than those of a metal. Thus, it is not surprising that all photoemitters of practical importance are semiconducting materials.

In recent years, remarkable improvements in the photoemission from semiconductors have been obtained through deliberate modification of the energy-band structure. The approach has been to reduce the electron affinity, E_A, and thus to permit the escape of electrons which have been excited into the conduction band at greater depths within the material. Indeed, if the electron affinity is made less than zero (the vacuum level lower than the bottom of the conduction band, a condition described as "negative electron affinity" and illustrated in Fig. 3), the escape depth may be as much as 100 times greater than for the normal material. The escape depth of a photoelectron is limited by the energy loss suffered in phonon scattering. Within a certain period of time, of the order of 10^{-12} second, the electron energy drops from a level above the vacuum level to the bottom of the conduction band from which it is not able to escape into the vacuum. On the other hand, the electron can stay in the conduction band in the order of 10^{-10} second without further loss of energy, i.e., without dropping into the valence band. If the vacuum level is below the bottom of the conduction band, the electron will be in an energy state from which it can escape into the vacuum for a period of time that is approximately 100 times longer than if an energy above the bottom of the conduction band is required for escape, as in the materials represented by Fig. 2. Therefore, a material conforming to the conditions of Fig. 3 has a greatly increased escape depth. Under such circumstances, the photosensitivity is significantly enhanced. Substantial response is observed even for photons with energies close to that of the band gap where the absorption is weak. Efficient photoemission in this case results only because of the greater escape depth.

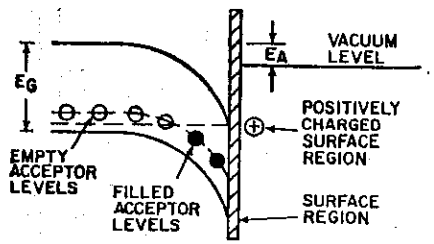

Fig. 3 — Semiconductor energy-band model showing negative electron affinity.

The reduction of the electron affinity is accomplished through two steps. First, the semiconductor is made strongly p-type by the addition of the proper "doping" agent. For example, if gallium arsenide is the host material, zinc may be incorporated into the crystal lattice to a concentration of perhaps 1,000 parts per million. The zinc produces isolated energy states within the forbidden gap, near the top of the valence band, which are normally empty, but which will accept electrons under the proper circumstances. The p-doped material has its Fermi level near the top of the valence band. The second step is to apply to a semiconductor a surface film of an electropositive material such as cesium. Each cesium atom becomes ionized through loss of an electron to a p-type energy level near the surface of the semiconductor, and is held to the surface by electrostatic attraction.

The changes which result in the energy-band structure are two-fold. In the first place, the acceptance of electrons by the p-type impurity levels is accompanied by a downward bending of the energy bands. This bending can be understood by observing that a filled state must be, in general, below the Fermi level; the whole structure near the surface is bent downward to accomplish this result. In the second place, the potential difference between the charged electropositive layer (cesium) and the body charge (filled zinc levels) results in a further depression of the vacuum level as a result of a dipole moment right at the surface.

Another way to describe the reduction of the electron affinity is to consider the surface of the semiconductor as a capacitor. The charge on one side of the capacitor is represented by the surface layer of cesium ions; the other charge is represented by the region of filled acceptor levels. The reduction in the electron affinity is exactly equal to the potential difference developed across the capacitor.

In a more rigorous analysis, the amount by which the energy bands are bent is found to be approximately equal to the band-gap, and the vacuum level is lowered until the absorption level of the electropositive material is essentially at the top of the valence band.

Measurements of Photocathode Sensitivity

There are various ways of specifying the sensitivity of a photocathode. For many purposes, a knowledge of the response of the photocathode to particular wavelengths or equivalent energies of radiation is necessary. Sometimes it is convenient to have

parent photocathode deposited upon its inner surface. The photocathode emits photoelectrons by the process of photoemission, i.e., by the interaction of the incident radiant energy with electrons in the photocathode material. Photoelectrons from all parts of the photocathode are accelerated by an electric field so as to strike a small area on the first dynode. Secondary electrons resulting from the process of secondary emission (i.e., from the impact of the photoelectrons on the first dynode) are accelerated toward the second dynode by an electric field between dynodes No. 1 and No. 2 and impinge on the second dynode. The impact of the secondary electrons on dynode No. 2 results in the release of more secondary electrons which are then accelerated toward dynode No. 3. This process is repeated until the electrons leaving the last dynode are collected by the anode and leave the photomultiplier as the output signal. If, on the average, 4 secondary electrons are liberated at each dynode for each electron striking that dynode, the current amplification for a 12-stage photomultiplier is 4^{12}, or approximately 17 million. Thus, the liberation of a single photoelectron at the photocathode results in 17 million electrons being collected at the anode. Because this pulse has a time duration of approximately 5 nanoseconds, the anode current is approximately 1 milliampere at the peak of the anode-current pulse.

PHOTOEMISSION AND PHOTOCATHODES

Photoemission is a process in which electrons are liberated from the surface of a material by the interaction of photons of radiant energy with the material.[1] The energy of a photon E_p is given by

$$E_p = h\nu = \frac{hc}{\lambda} \qquad (1)$$

where ν is the frequency of the incident radiation, λ is the wavelength of the incident radiation, h is Planck's quantum of action, and c is the velocity of light. Substitution of the numerical values of these constants from Appendix A provides the following relation:

$$E_p = \frac{1239.5}{\lambda} \qquad (2)$$

where E_p is in electron-volts and λ is in nanometers. Thus, photons of visible light which are in the wavelength range from 400 to 700 nanometers have energies ranging from 3.1 to 1.8 electron-volts.

Fundamentals of Photoemission

An ideal photocathode has a quantum efficiency of 100 per cent; i.e., every incident photon releases one photoelectron from the material into the vacuum. All practical photoemitters have quantum efficiences below 100 per cent. To obtain a qualitative understanding of the variations in quantum efficiency for different materials and for different wavelengths or photon energies, it is useful to consider photoemission as a process involving three steps: (1) absorption of a photon resulting in the transfer of energy from photon to electron, (2) motion of the electron toward the material-vacuum interface, and (3) escape of the electron over the potential barrier at the surface into the vacuum.

Energy losses occur in each of these steps. In the first step, only the absorbed portion of the incident light is effective and thus losses by transmission and reflection reduce the quantum efficiency. In the second step, the photoelectrons may lose energy by collision with other electrons (electron scattering) or with the lattice (phonon scattering). Finally, the potential barrier at the surface (called the work function in metals) prevents the escape of some electrons.

The energy losses described vary from material to material, but a major difference between metallic and semiconducting materials makes separate consideration of each of these two groups useful. In metals, a large fraction of the incident visible light is reflected and thus lost to the photoemission process. Further losses occur as the photoelectrons rapidly lose energy in collisions with the large number of free electrons in the metal through electron-electron scattering. As a result, the escape depth, the distance from the surface from which electrons can reach the surface with sufficient energy to overcome the surface barrier, is small, and is typically a few nanometers. Finally, the work function of most metals is greater than three electron-volts, so that visible photons which have energies less than three electron-volts are prevented from producing electron emission. Only a few metals, particularly the alkali ones, have work-function values low enough to make them sensitive to visible light. Because of the large energy losses in absorption of the photon and in the motion of the photoelectron toward the vacuum (the first and second steps described above), even the alkali metals exhibit very low quantum efficiency in the visible region, usually below 0.1 per cent (one electron per 1000 incident photons). As expected, higher quantum efficiencies are obtained with higher photon energies. For 12-electron-volt photons, quantum yields as high as 10 per cent have been reported.

The concept of the energy-band models that describe semiconductor photoemitters is illustrated in its simplest form in Fig. 2. Electrons can have energy values only within well defined energy bands which are separated by forbidden-band gaps.

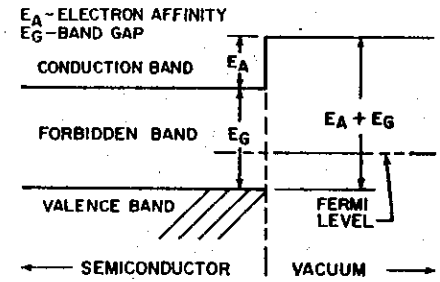

Fig. 2 — Simplified semiconductor energy-band model.

At 0°K, the electrons of highest energy are in the so-called valence band and are separated from the empty conduction band by the band-gap energy E_G. The probability that a given energy level may be occupied by an electron is described by Fermi-Dirac statistics and depends primarily on the difference in energy between the level under consideration and a reference level called the "Fermi level." As a first approximation, it may be said that any energy levels which are below the Fermi level will be filled with electrons, and any levels which are above the Fermi level will be empty. At temperatures higher than 0°K, some electrons in the valence band have sufficient energy to be raised to the conduction band, and these electrons, as well as the holes in the valence band created by the loss of electrons, produce electrical conductivity. Because the number of electrons raised to the conduction band increases with temperature, the conductivity of semiconductors also increases with temperature. Light can be absorbed by valence-band electrons only if the photon energy of the light is at least

vent of the bialkali photocathode and more recently the Extended Red Multi-Alkali (ERMA) photocathode provided further improvements. Very recently, advances in solid-state theory and semiconductor-materials research have opened new vistas in the development of photomultipliers having performance capabilities that were literally impossible only a few years ago.

REFERENCES

1. J. Slepian, U. S. Patent 1,450.-265, April 3, 1923 (Filed 1919).
2. H. Iams and B. Salzberg, "The Secondary-Emission Phototube," *Proc. IRE, Vol. 23,* pp. 55–64 (1935).
3. J. A. Rajchman and R. L. Snyder, "An Electrostatically-Focused Multiplier Phototube," *Electronics, Vol. 13,* p. 20 (1940).
4. P. T. Farnsworth, "An Electron Multiplier," *Electronics, Vol. 7,* pp. 242–243 (1934).
5. V. Zworykin, G. Morton, and L. Malter, "The Secondary-Emission Multiplier—A New Electronic Device," *Proc. IRE, Vol. 24,* pp. 351–375 (1936).
6. G. Weiss, "On Secondary-Electron Multipliers," *Z. f. Techn. Physik, Vol. 17,* No. 12, pp. 623–629 (1936).
7. W. Kluge, O. Beyer, and H. Steyskal, "Photocells with Secondary-Emission Amplification," *Z. f. Techn. Physik, Vol. 18,* No. 8, pp. 219–228 (1937).
8. J. R. Pierce, "Electron-Multiplier Design," *Bell Lab. Record, Vol. 16,* pp. 305–309 (1938).
9. V. K. Zworykin and J. A. Rajchman, "The Electrostatic Electron Multiplier," *Proc. IRE, Vol. 27,* pp. 558–566 (1939).
10. C. C. Larson and H. Salinger, "Photocell Multiplier Tubes," *Rev. Sci. Instr., Vol. 11,* pp. 226–229 (1940).
11. R. C. Winans and J. R. Pierce, "Operation of Electrostatic Photomultipliers," *Rev. Sci. Instr., Vol. 12,* pp. 269–277 (1941).
12. R. W. Engstrom, "Multiplier Phototube Characteristics; Application to Low Light Levels," *J. O. S. A., Vol. 37,* No. 6, pp. 421–431 (1947).

Photoemission and Secondary Emission

THIS section covers the means by which radiant energy is converted into electrical energy in a photomultiplier tube.

Photomultipliers convert incident radiation in the visible, infrared, and ultraviolet regions into electrical signals by use of the phenomenon of photoemission and then amplify the signals by means of secondary emission.

A basic component arrangement of a typical modern photomultiplier is shown in Fig. 1. Radiant energy enters the evacuated enclosure through a "window" which has a semitrans-

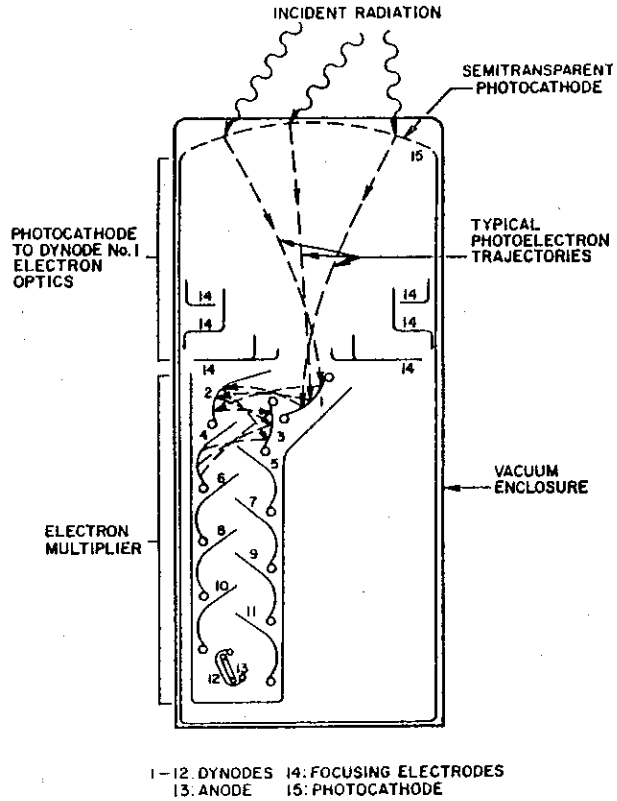

Fig. 1 — Schematic of typical photomultiplier showing some electron trajectories.